

1 **Numerical evaluation of the effectiveness of flexible joints in buried**
2 **pipelines subjected to strike-slip fault rupture**

3
4
5 **Vasileios E. Melissianos***

6 Institute of Steel Structures, School of Civil Engineering
7 National Technical University of Athens
8 9, Iroon Polytechneiou str., Zografou Campus
9 GR-15780, Athens, Greece
10 email: melissia@mail.ntua.gr
11 tel: +302107722553

12
13 **Georgios P. Korakitis**

14 Institute of Steel Structures, School of Civil Engineering
15 National Technical University of Athens
16 9, Iroon Polytechneiou str., Zografou Campus
17 GR-15780, Athens, Greece
18 email: geo.korakitis@gmail.com

19
20 **Charis J. Gantes**

21 Institute of Steel Structures, School of Civil Engineering
22 National Technical University of Athens
23 9, Iroon Polytechneiou str., Zografou Campus
24 GR-15780, Athens, Greece
25 email: chgantes@central.ntua.gr
26 tel: +302107723440

27
28 **George D. Bouckovalas**

29 Department of Geotechnical Engineering, School of Civil Engineering
30 National Technical University of Athens
31 9, Iroon Polytechneiou str., Zografou Campus
32 GR-15780, Athens, Greece
33 email: gbouck@central.ntua.gr
34 tel: +3021077223780

35
36
37
38
39
40
41
42
43
44
45
46
47
48
49
50 *Corresponding author additional contact: melissianosv@gmail.com

51 **KEYWORDS:** buried pipeline, seismic fault, numerical model, flexible joints

52

53 **ABSTRACT**

54 Buried steel pipelines transport large amounts of fuel over long distances and inevitably
55 cross active tectonic seismic faults when seismic areas are traversed. Eventual fault
56 activation leads to large imposed displacements on the pipeline, which may then fail due to
57 local wall buckling or tensile weld fracture, having grave financial, social and environmental
58 consequences. In this paper, flexible joints are evaluated as an innovative mitigating
59 measure against the consequences of faulting on pipelines. Joints are introduced in the
60 pipeline in the fault vicinity, aiming at absorbing the developing deformation through relative
61 rotation between adjacent pipeline parts, which then remain relatively unstressed. The
62 effectiveness of flexible joints is numerically evaluated through advanced 3D nonlinear finite
63 element modeling. Extensive parametric analysis is carried out to determine the effect of
64 pipeline – fault crossing angle, fault offset magnitude, joint angular capacity, burial depth and
65 diameter over thickness ratio on the joint efficiency. The uncertainty regarding the fault trace
66 is also addressed.

67

68

69

70

71

72

73

74

75

76

77

78

79 1. INTRODUCTION

80 Onshore buried steel pipelines with girth-welded joints are used in the energy industry
81 to transport large amounts of fuel over long distances. Permanent ground displacements
82 (PGD), such as those due to fault rupture, ground settlement or sloping ground failure, have
83 been identified as the dominant causes of catastrophic pipeline failure due to earthquake
84 induced actions after past major earthquake events [1] (e.g. the 1995 Kobe [2], the 1999
85 Kocaeli [3] and the 1999 Chi-Chi [4] earthquakes). A potential failure of pipelines (e.g. fuel
86 leakage, explosion) can have significant environmental and financial consequences. Fault
87 offset is the result of earth plate's relative movement and its consequences on pipeline
88 performance can be severe. The principal failure modes in this case are directly related to
89 the extensive deformation of pipelines due to faulting causing local buckling/wrinkling due to
90 compressive strains or tensile weld fracture due to tensile strains.

91 Analytical or numerical approaches have been applied to assess the pipe stress-state
92 due to faulting. Newmark and Hall [5] analytically calculated the pipeline wall stress-state,
93 considering the pipeline as a long cable undergoing small displacements that intercepts a
94 planar fault. Kennedy et al. [6],[7] extended previous work [5] by incorporating lateral soil
95 interaction and pipe – soil friction nonlinearity. Wang and Yeh [8] integrated the pipe bending
96 stiffness in the established analytical models. The pipe model of elastic beam was adopted
97 by Vougioukas et al. [9] to account for the vertical and horizontal fault movements. Wang
98 and Wang [10] modeled the pipe as a beam on elastic foundation, while Takada et al. [11]
99 proposed a more accurate model by relating the cross-sectional deformation and the pipe
100 bending angle to calculate the maximum strain. Recently, Karamitros et al. [12],[13]
101 improved the previous analytical approaches by combining the model of a beam on elastic
102 foundation and the elastic beam theory to estimate the maximum strains due to strike-slip
103 and normal faulting. Trifonov and Cherniy [14],[15] presented a semi-analytical methodology
104 for pipeline stress – strain analysis by considering the contribution of transverse
105 displacements to the axial elongation.

106 The analytical approach remains a helpful tool during the preliminary design stage of a
107 pipeline project. The pipeline – soil interaction complexity, however, requires the
108 implementation of advanced numerical models that are capable of considering all pertinent
109 parameters, such as geometrical and material nonlinearity, cross-section ovalization and
110 complex soil properties. The finite element method was initially introduced [16] to evaluate
111 the developing strains and nowadays two categories of numerical models are available:

112 • The first is the so-called beam-type model, where the pipeline is meshed with beam-type
113 finite elements that can model the axial, shear and bending deformation and can provide
114 stresses and strains at cross-section integration points along the pipe. The surrounding
115 soil is modeled using a series of nonlinear translational springs in four directions (axial,
116 transverse horizontal, transverse vertical upward and downward), based on the Winkler
117 soil approach. However, trench dimensions and native soil properties cannot be directly
118 encountered in the analysis. Additionally, the used of beam-type finite elements does not
119 allow the direct estimation of local buckling, cross-section ovalization and detailed stress-
120 strain distributions around the circumference of the pipe. Thus, checks on failure modes
121 are carried out by comparing the maximum developing tensile and compressive strains
122 obtained from the integration points to the corresponding strain limits provided by
123 pertinent standards. The beam-type model is extensively used by researchers to verify
124 the pipeline safety at active fault crossings. Joshi et al. [17] employed this model to
125 investigate the pipe behavior due to reverse faulting. Uckan et al. [18] presented a
126 simplified beam-type model as a useful tool to calculate the pipe critical length and
127 established a methodology to formulate pipe fragility curves. This model is also adopted
128 by worldwide Standards and Regulations such as Eurocode 8 [19], ALA [20] and ASCE
129 [21] as a reliable and computationally efficient modeling approach.

130 • The second approach is the so-called continuum model, where the pipeline is discretized
131 into shell finite elements and the surrounding soil into 3D solid elements. The pipe – soil
132 interaction is modeled with contact elements. This approach severely increases modeling
133 complexity, nonlinearity and computational effort in terms of solution time requirements,

134 boundary conditions, resulting degrees of freedom, convergence difficulties, fault rupture
135 modeling and particularly the introduction of contact elements. The initial attempts to
136 employ the continuum model by considering pipe – soil contact issues were presented in
137 [22],[23]. Recently, Vazouras et al. [24],[25],[26] presented a rigorous finite element
138 model for pipeline – strike-slip fault crossing by considering soil parameters, pipe – fault
139 crossing angle and pipeline mechanical characteristics to come up with a simplified
140 expression for critical buckling strain. This model was then adopted in [27],[28] to
141 consider the effects of trench dimensions, native soil properties and fault motion
142 simulation. As an alternative, nonlinear translation springs can be used for soil modeling
143 instead of 3D-solid elements to avoid the numerical difficulties related to the use of
144 contact elements between the pipeline and the soil [12],[13],[29],[30].

145 Avoiding pipeline failure is the major priority in pipeline design against faulting. A set of
146 different seismic countermeasures are thus employed in engineering and constructional
147 practice to minimize the developing strains on pipe walls, mainly by reducing pipe – soil
148 reaction forces. The commonly adopted measures are:

- 149 • Pipeline embedment in a shallow, sloped-wall trench with loose backfill to reduce soil
150 resistance and allow the pipeline deformation to take place over a longer length.
151 Development of large strains and permanent deformations is allowed, as long as pipe
152 failure is prevented [30],[31].
- 153 • Pipe wall thickness increase or steel grade upgrade to reduce developing strains and
154 pipe curvature by increasing pipe stiffness [30],[31].
- 155 • Avoidance of sharp bends that increase constraints to axial displacements and may
156 impose additional forces on the pipeline [19],[20],[30].
- 157 • Pipeline wrapping with friction-reducing geotextile to reduce pipe – soil friction and
158 increase the anchor length, thus reducing the developing longitudinal strains [30].
- 159 • Pipeline wrapping with composite FRP wraps to increase strength and the critical fault
160 movement that causes failure [32].

- 161 • Pipeline placement within buried concrete culverts. Culverts are sacrificed during the fault
162 movement to retain the pipeline unstressed. The lack of backfilling drastically reduces
163 friction-induced strains on the pipeline.
- 164 • Use of geocells and geogrids in the trench above the pipeline to reduce pipe deformation
165 [33].
- 166 • Backfill pipe trench with tyre derived aggregate surrounded by sand to reduce pipe
167 bending moments [34].

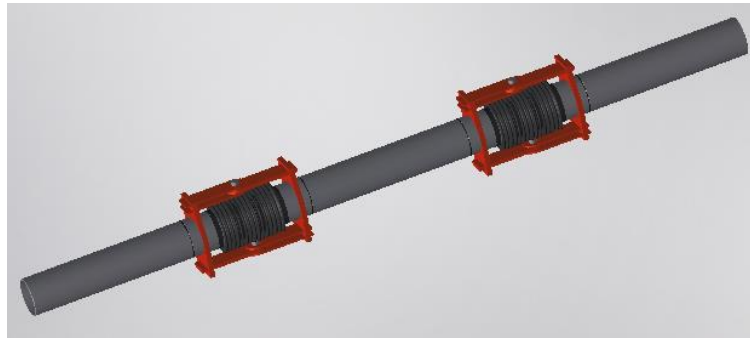
168 Various parameters, such as the fault offset magnitude and constructional issues, can
169 limit the efficiency of these measures. Monroy [35] for example, suggests that wrapping the
170 pipeline with a double layer geotextile is effective only if the distance between pipeline and
171 trench wall is less than half the pipeline diameter.

172 Research presented in the present paper focuses on the use of innovative materials or
173 commercial devices/products that could be integrated in the pipeline in the fault vicinity in
174 order to reduce the developing strains. Segmented pipelines have been used in the piping
175 industry for decades, but mainly for water or sewage transmission under low pressure. The
176 joints used in these pipelines (slip and spigot-bell joints) do not ensure the continuity of the
177 structure in terms of axial, shear and/or rotational deformations, depending on the type of
178 joint, and thus extensive research has been carried out on investigating the integrity of
179 segmented pipelines under permanent ground displacements based on the joints' properties
180 [36]-[44], investigating among others the potential of joint pull-out failure. The mitigation
181 measure proposed in the present study follows the suggestions of Bekki et al. [45] in
182 introducing flexible joints between the adjacent pipeline parts in the fault crossing area. The
183 principal objective is to concentrate strains at the joints and retain the steel parts almost
184 undeformed [46],[47]. This concept introduces a different design approach for reducing the
185 risk of local buckling or tensile failure, by transforming the pipeline structural system from
186 continuous to segmented, so as to concentrate strains at the joints, instead of reducing the
187 soil friction.

188 Flexible joints are widely used in the piping industry, for example to absorb thermal
189 expansion, thrust and machinery vibration or as joints between the adjacent parts of
190 segmented pipelines. A major advantage is that flexible joints are commercial products, thus
191 they can be either readily available or also customized with respect to diameter, internal
192 pressure and allowable deformations. Among the available flexible joints, namely slip joints,
193 spigot-bell joints and bellows, it was concluded that the appropriate type for buried pipe
194 applications that operate in high pressure is the hinged metallic bellow (Fig. 1), which is
195 capable of undergoing angular deformation only, as lateral and axial movements are
196 restrained. The selection is based on the following criteria: (i) availability in the market and
197 production upon request, (ii) contribution to developing longitudinal strain reduction, (iii) ease
198 of construction in the field, (iv) compliance with pipe flow, (v) operability of pipeline after fault
199 rupture and (vi) full structural cooperation between the pipe and the flexible joint, i.e.
200 avoidance of joint pull-out failure. Focus on the latter is important due to the fact that bellow-
201 type joints are welded between the pipeline segments and thus continuity of the structure is
202 ensured. It is also noted that the integrated joints are expected to undergo large rotations
203 due to fault offset and thus joint rotations have been quantified for a wide range of values of
204 the involved parameters, indicating that there are commercially available bellow-type joints
205 with sufficient rotational capacity to accommodate the required rotation for very large offsets,
206 in the order of 3 to 4 pipe diameters. Almost all alternative protection measures are not
207 effective for such large offsets.

208 Transmission pipelines operate usually under very high pressure (e.g. 8 MPa) that
209 may deform heavily a single joint in normal operation, while hinged joints can withstand high
210 pressure. It is noted that hinged metallic bellows have not been used until now in high-
211 pressure buried pipeline – fault crossing applications. In the market, however, hinged joints
212 for high pressure are available. Therefore, the use of expansion joints in such applications
213 has to be accompanied by special procedures and precautions regarding pipe – joint
214 welding, joint corrosion, thermal insulation, joint protection against external damage,
215 compliance with the pipe flow process, avoidance of obstructing the normal pipeline

216 inspection procedures (e.g. in-line inspection with pigs) and joint angular capacity with
217 respect to the expected fault offset magnitude.



218
219 Figure 1: Schematic illustration of the introduction of hinged flexible joints in a pipeline

220 The research objective of this paper is the evaluation of the mechanical behavior of
221 buried pipelines with flexible joints subjected to fault rupture and the demonstration of the
222 advantages of flexible joints as mitigating measures against the consequences of faulting in
223 terms of reducing the risk of pipe failure, provided that the technological and practical
224 aspects of such joints are solved. Pipelines with flexible joints behave as segmented pipes
225 under fault rupture and the response is characterized by rotations at the joints and small
226 deformation of the parts between the pipes. However, the relative values of pipe – joint – soil
227 stiffness render their actual response unknown and thus different parameters affecting the
228 mechanical behavior due to faulting are examined, to identify the optimum range within
229 which joints reduce the risk of pipeline failure. The study is carried out numerically through
230 advanced nonlinear analyses.

231

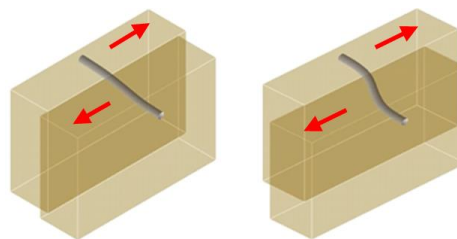
232 **2. PIPELINE – FAULT CROSSING**

233 **2.1 Details of pipeline finite element model**

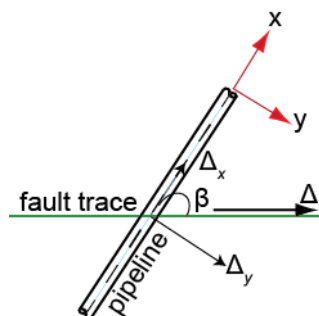
234 Among the two alternative pipeline modeling techniques, i.e. beam-type and
235 continuum model, the beam-type model is more appropriate for practical applications, taking
236 also into account the fact that several fault crossings will be encountered by a single pipeline
237 traversing a seismic area, hence a large number of analyses will be required. Time and
238 computational cost requirements can be significant parameters determining the acceptability

239 of the continuum model by design engineers. The beam-type model is adopted hereinafter to
240 investigate the mechanical behavior of continuous pipelines and pipelines with flexible joints
241 to demonstrate the effectiveness of flexible joints in protecting buried pipelines against PGD.

242 The behavior of pipelines subjected to strike-slip fault movement is addressed, hence
243 the pipeline deformation is assumed to take place within a horizontal plane. Schematic
244 illustration of two successive stages of pipeline deformation subjected to strike-slip faulting is
245 presented in Fig. 2. A planar fault with zero thickness is considered in the analysis, crossing
246 a straight pipeline segment at the middle of its modeled length. The pipeline stress-state is
247 directly related to the pipe – fault crossing angle β whose selection is related among others
248 to the route selection procedure, seismological and geotechnical aspects of the seismic fault
249 and the expected fault offset. Crossing angles $\beta \leq 90^\circ$ lead to pipeline bending and tension,
250 while angles $\beta > 90^\circ$ lead to bending and compression [48] and their effect will be discussed
251 later. Fault displacement Δ is parallel to the fault trace and is decomposed to the imposed
252 pipeline displacements with respect to the crossing angle β : Δ_x along the pipeline axis and Δ_y
253 perpendicular to the pipeline axis (Fig. 3).



254
255 Figure 2: Schematic illustration of two successive stages of pipeline deformation due to
256 strike-slip faulting



257
258 Figure 3: Pipeline – fault crossing site plan view

259 Pipeline numerical modeling is carried out using the general purpose finite element
260 software ADINA [49]. The pipe is discretized into PIPE elements that are Hermitian 2-node
261 beam-type finite elements with extra degrees of freedom to account for cross-section
262 ovalization. A longitudinal mesh density equal to 0.25 m is selected after a mesh density
263 sensitivity analysis is performed to define the optimum length of pipe elements with respect
264 to accuracy and computational cost efficiency. Geometrical nonlinearity is considered in the
265 analysis to account for the second order effects resulting from potential fault activation in the
266 order of meters and cross-section ovalization. Soil modeling is carried out using discrete
267 springs after ALA [20] provisions (Fig. 4). Elastic – perfectly plastic soil springs are modeled
268 in ADINA using nonlinear SPRING elements that exhibit stiffness only in the local axial
269 direction and connect pipe nodes to “ground” nodes. Soil “ground” nodes on the fault footwall
270 are considered fixed, while the corresponding ones on the fault hanging wall are subjected to
271 the imposed displacement caused by the fault movement. Non-seismic and in service
272 actions (e.g. internal pressure, corrosion, overburden soil weight, hydraulic transient actions,
273 etc.) are not considered in the present study.

274 Flexible joints can be modeled either as a general beam-type finite element with its
275 stiffness matrix being constructed from the spring rates provided by the manufacturer, or as
276 a generic flexible joint, represented by a rotational spring at the center point, without
277 considering the joint length [50]. The second modeling approach for the joint has been
278 adopted in the present study, namely by simulating the joint with a rotational spring, while
279 the joint lateral and axial relative movements at the two ends are restrained. The joint
280 torsional movement is generally prohibited by the manufacturers [51] and thus rotation about
281 the longitudinal axis is restricted through appropriate constraints.

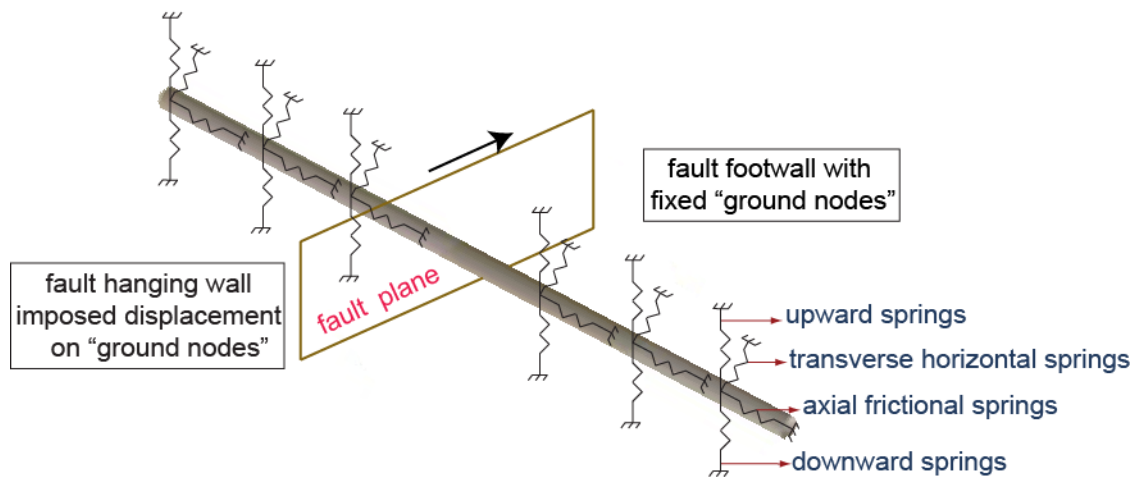


Figure 4: Beam-type finite element model of pipeline – fault crossing

The imposed displacements caused by fault movement evolve at an adequately slow rate that allows the engineer to neglect any dynamic phenomena, considering the fault offset as a quasi-static process [19],[20], [48]. Accordingly, fault rupture is treated herein as a static phenomenon. The problem's inherent nonlinearity is handled through the implementation of the Newton-Raphson or Arc-Length solution algorithms [52]. Numerical convergence and smooth displacement application are achieved by selecting a proper number of analysis steps so that the external loading application follows closely the response evolution.

A typical high-pressure, large diameter natural gas pipeline is considered as a case study. The pipe's modeled length is 1000 m, following a sensitivity analysis to define a sufficient length within which the soil reactions have vanished. The cross-section is of diameter $D = 914$ mm (36 in) and thickness $t = 12.7$ mm (0.5 in). Material nonlinearity is considered through an elastic – plastic bilinear law with isotropic hardening. Steel is of type API5L-X65 with the properties listed in Table 1. While pipeline steel is commonly modeled via the Ramberg-Osgood formula, in the present study nonlinear material modeling is actually of very minor importance, taking into account that the response of buried pipelines with flexible joints is well into the elastic range, as will be shown in the subsequent sections.

303

Table 1: API5L-X65 steel properties

Property	Value
Elastic Young's modulus (GPa)	210
Plastic Young' modulus (GPa)	0.464
Yield stress (MPa)	448.5
Yield strain (%)	0.214
Failure stress (MPa)	510
Failure strain (%)	18

304

305 The pipeline is assumed to be coal-tar coated and embedded under 1.30 m of granular
306 loose sand with unit weight $\gamma = 18\text{kN/m}^3$, cohesion $c = 0$ and internal friction angle $\phi = 36^\circ$.
307 The corresponding soil spring properties are estimated according to ALA provisions [20] and
308 are listed in Table 2. Finally, flexible joints introduced in the pipeline exhibit rotational
309 stiffness equal to 100 kNm/rad and angular capacity equal to 40° (e.g. [53],[54]). Note that in
310 case of large diameter and high-pressure pipeline, excessive flexible joint rotation may be
311 undesirable, as it may cause flow disruption.

312 Table 2: Soil spring properties

Spring type	Yield force (kN/m)	Yield displacement (mm)
Axial (friction)	40.69	3
Transverse horizontal	320.07	23
Vertical (upward displacement)	45.46	4.6
Vertical (downward displacement)	1493.65	114

313

314 2.2 Pipeline failure modes

315 Pipeline design against permanent ground displacements is carried out in strain terms,
316 rather than stress terms. Strain Based Design (SBD) is the appropriate design approach in
317 cases where stresses and strains are expected to exceed the proportional limit and the
318 external loading is displacement-controlled. The SBD possesses a major advantage: when
319 strain and stress are not proportional, stress-based methods may become very sensitive to
320 the details of the material stress – strain behavior and to any safety factors. Codes and
321 standards therefore adopt strain limits to evaluate the potential of the two main pipe failure
322 modes:

323 (a) Tensile strains may rupture the pipeline wall at areas of strain concentration or defected
324 locations. Areas of great concern are the girth welds between the adjacent pipeline parts,
325 given that the pipeline is corrosion and defect free. Eurocode 8 [19] suggests a tensile
326 limit of 5%, while ALA [20] an operable limit of 2% and a pressure integrity limit of 4%.
327 However, taking also into account the concern regarding the integrity of girth welds and
328 their capability to develop such high strains due to the metallurgical alterations induced by
329 the steel heat-affected zone during the welding procedure, a suggestion in engineering
330 practice is to further lower the tensile limit conservatively to 0.5% [30]. In the present
331 study the code-based tensile limit of 2% by ALA is adopted.

332 (b) Compressive strains can cause local buckling of the pipeline wall and consequently lead
333 to leak or rupture. Strain concentration leads to the formation of a wrinkle that extends
334 over a short pipe length. The wrinkle then evolves to a local buckle as compression
335 increases. Local buckling is handled by codes and standards as an ultimate limit state
336 and compressive strain limit expressions are provided to avoid this critical condition. The
337 ALA [20] operable limit is adopted here:

$$338 \quad \varepsilon_c = 0.50 \left(\frac{t}{D'} \right) - 0.0025, \text{ with } D' = \frac{D}{1 - 3 \frac{D - D_{\min}}{D}} \quad (1)$$

339 where t is the pipe wall thickness, D the external diameter, E the pipe steel elastic
340 modulus and D_{\min} the pipe minimum inside diameter. The compressive strain limit equals
341 0.39%, after Eq. (1), for the pipeline under investigation.

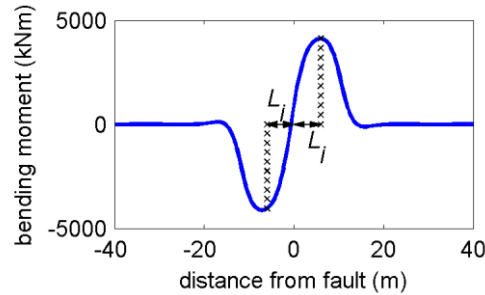
342

343 **3. NUMERICAL ANALYSIS RESULTS**

344 **3.1 Investigation of optimum number and locations of flexible joints**

345 The primary consideration in adopting flexible joints as mitigating measures is to
346 determine the optimum number and locations of the joints that minimize the cost and
347 maximize the efficiency in terms of preventing failure through strain reduction. The joint
348 locations are initially selected based on the bending moment distribution of the continuous

349 pipeline caused by faulting, given that joints act as internal hinges in the structural system.
 350 Specifically, primary candidate locations for joints are the sections of maximum bending
 351 moment of the continuous pipeline on either sides of the fault trace. The distance between
 352 the maximum bending moment location and the fault trace is defined as L_j (Fig. 5). In strike-
 353 slip fault type the bending moment distribution is antisymmetric due to the symmetric lateral
 354 soil resistance. At this stage the uncertainty regarding the fault trace is disregarded.



355
 356 Figure 5: Definition of L_j length in bending moment distribution of a continuous pipeline

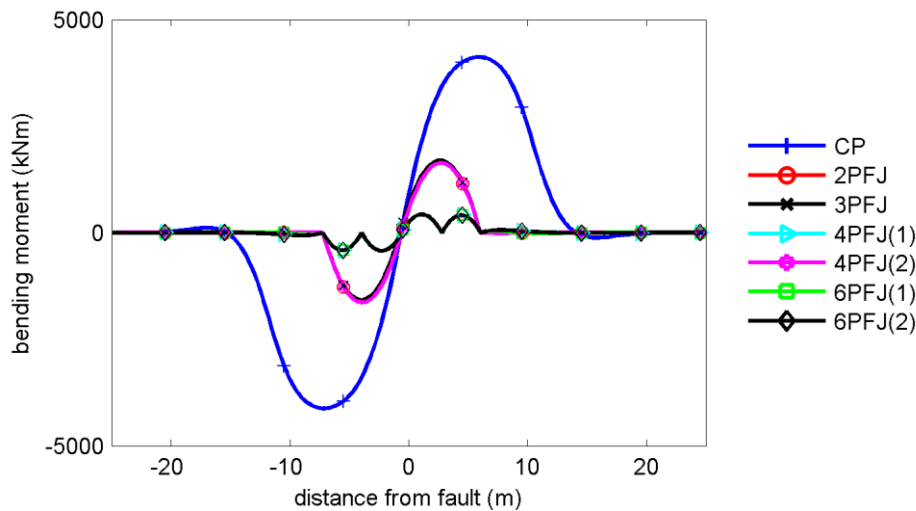
357 To investigate the best combination of joints, six different cases of pipes with joints are
 358 investigated with respect to length L_j (Table 3). Throughout this study, the continuous
 359 pipeline is abbreviated as CP and the pipeline with flexible joints as PFJ. The pipelines are
 360 assumed to intercept a strike-slip fault with crossing angle $\beta = 90^\circ$ and subjected to fault
 361 offset magnitude of $\Delta/D = 2$. In the case under investigation the distance L_j equals 6.5 m.

362 Table 3: Cases of pipelines with flexible joints under investigation

Case	Number of joints	Joints location
2PFJ	2	$-L_j, +L_j$
3PFJ	3	$-L_j, 0, +L_j$
4PFJ(1)	4	$-L_j, -L_j/2, +L_j/2, +L_j$
4PFJ(2)	4	$-2L_j, -L_j, +L_j, +2L_j$
6PFJ(1)	6	$-3L_j/2, -L_j/2, -L_j, +L_j/2, +L_j, +3L_j/2$
6PFJ(2)	6	$-2L_j, -L_j, -L_j/2, +L_j/2, +L_j, +2L_j$

363
 364 The effectiveness of flexible joints for very significantly decreasing the bending
 365 moment in all PFJ cases is demonstrated in Fig. 6. It is noted that, for this crossing angle $\beta =$
 366 90° , the pipeline behavior is predominantly flexural, corresponding to optimum conditions for
 367 hinge-type flexible joints, as pipe axial strains are practically zero. The bending moment
 368 reduction with respect to the continuous pipeline is also quantified in Table 4, accompanied

369 also by the maximum rotations of all joints for all PFJ cases. The maximum moment
 370 reduction is reported in 4PFJ(1), 6PFJ(1) and 6PFJ(2) cases, while cases 2PFJ, 3PFJ and
 371 4PFJ(2) exhibit smaller reduction. In cases 4PFJ(2), 6PFJ(1) and 6PFJ(2) the joints that are
 372 located beyond L_j distance ($\pm 2L_j$ and $\pm 3L_j/2$) exhibit almost zero rotation, while joints located
 373 at $L_j/2$ in 4PFJ(1), 6PFJ(1) and 6PFJ(2) cases exhibits the same rotation, as well as joints at
 374 L_j in 2PFJ and 4PFJ(2) cases. Hence, the optimum case is 4PFJ(1), as joints located
 375 beyond L_j distance nearly do not rotate (shown also in Fig. 6) and consequently they are
 376 inactive. The case 4PFJ(1) of the pipeline with four joints located at distances L_j and $L_j/2$ on
 377 each side of the fault trace (abbreviated in the following for simplicity as PFJ) is hence
 378 adopted hereinafter to further investigate the parameters affecting the joint's efficiency.



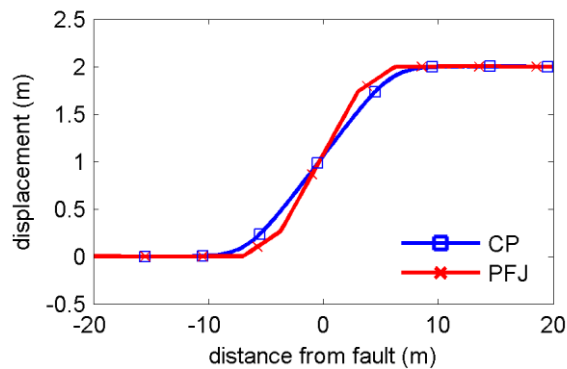
379
 380 Figure 6: Bending moment distributions of continuous pipeline and pipelines with flexible
 381 joints subjected to strike-slip faulting

382 Table 4: Maximum bending moment reduction with respect to the continuous pipeline and
 383 joint rotation in all cases of pipelines with flexible joints

Case	Number of joints	Bending moment reduction (%)	Maximum joint rotation (°)
2PFJ	2	60.29	8.39
3PFJ	3	59.86	8.24
4PFJ(1)	4	89.64	8.10
4PFJ(2)	4	60.29	8.39
6PFJ(1)	6	89.64	8.10
6PFJ(2)	6	89.64	8.10

385 3.2. Response features of pipeline with flexible joints

386 The introduction of flexible joints in a buried steel pipeline modifies the structural
387 system from continuous to segmented. In order to evaluate and quantify this effect, the
388 continuous pipeline (CP) and the pipeline with four flexible joints (PFJ), as obtained from
389 section 3.1, are examined in more detail. The pipeline displacements are plotted in Fig. 7,
390 indicating a smooth curved shape for CP, while PFJ follows a piece-wise linear shape.
391 Furthermore, axial forces and bending moments are compared in Fig. 8.



392

393 Figure 7: CP and PFJ displacements

394 It is observed that the implementation of flexible joints leads to a very significant
395 decrease of bending moment (Fig. 8b), while a minor increase in axial force is observed (Fig.
396 8a). The pipeline response is dominated by bending and thus the hinged joints reduce
397 bending moment, while the axial force is marginally increased. The introduction of flexible
398 joints also leads to an important reduction of longitudinal maximum effective stresses, as
399 shown in Fig. 9. The stress distribution along the pipeline is symmetric around the fault trace,
400 given the strike-slip faulting and the symmetric soil response to any lateral pipeline
401 movement in the trench.

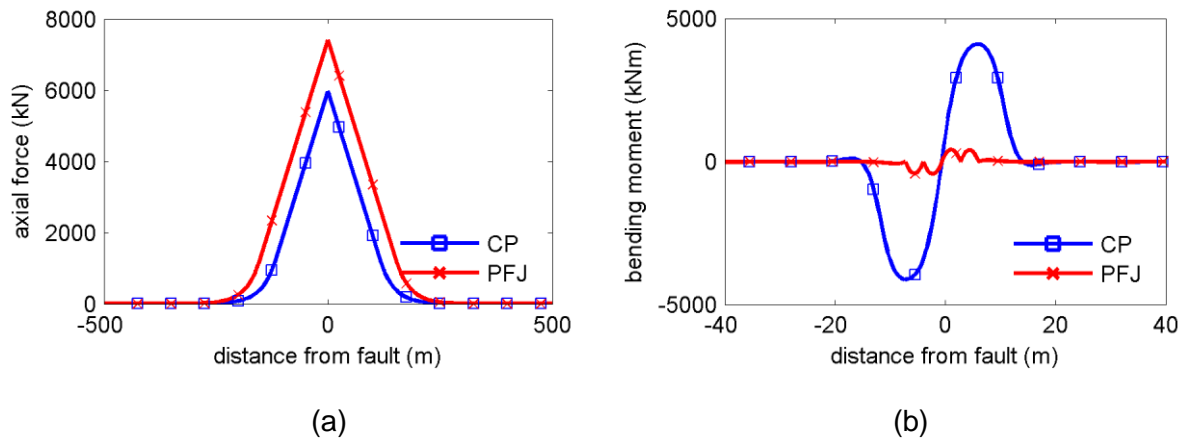


Figure 8: (a) Axial force and (b) bending moment distributions of CP and PFJ

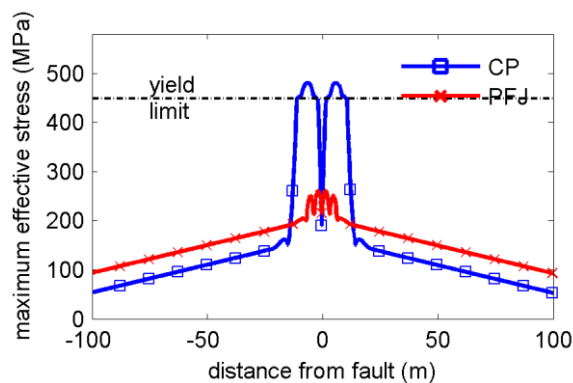
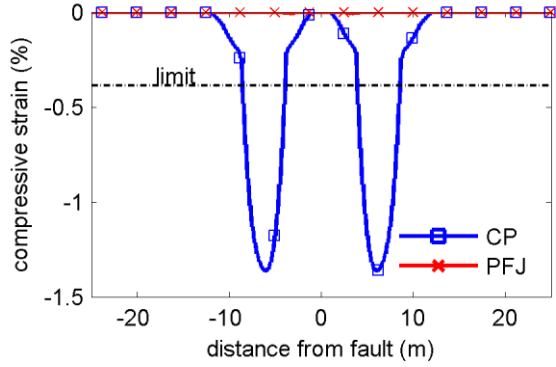
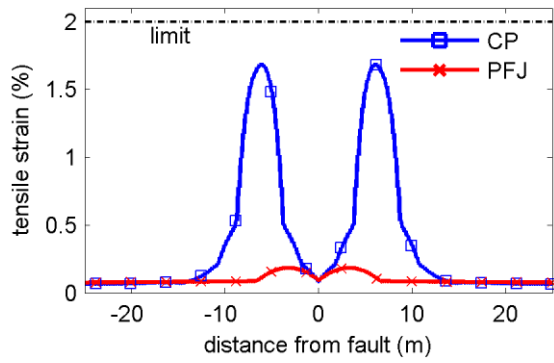


Figure 9: Maximum effective stress distributions along CP and PFJ

As the pipeline design against permanent ground displacements is carried out in strain terms, it is crucial to identify the PFJ response in terms of developing longitudinal strains, which are the summation of axial and bending strains. The longitudinal tensile strains are illustrated in Fig. 10a and the compressive strains in Fig. 10b, respectively, both indicating that the flexible joints contribute decisively to a sharp decrease of strains, thus minimizing the potential of pipeline failure due to either tensile fracture or local buckling. The compressive strains are particularly reduced, practically vanishing. The strain reduction is explained by the structural system's modification from continuous to segmented, as strains are concentrated at the joints, retaining the steel pipe parts nearly undeformed. The longitudinal strain distributions (Fig. 10) in combination with axial force (Fig. 8a) and bending moment (Fig. 8b) distributions lead to the conclusion that bending strains are much higher than axial strains and thereby hinged joints are the appropriate joint type for strike-slip faults.



419

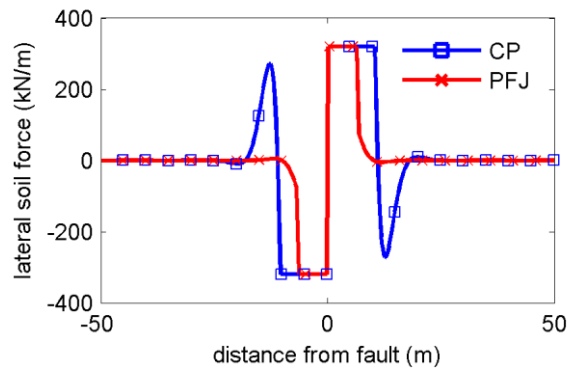
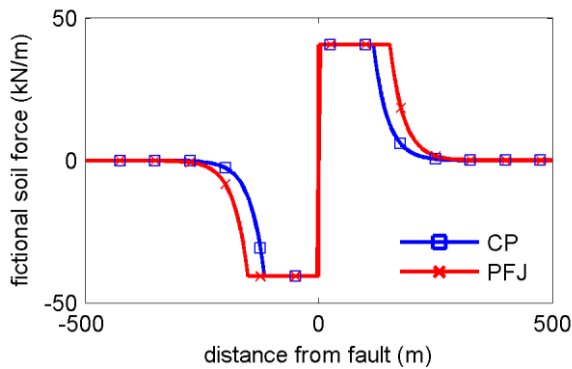
420

(a)

(b)

421 Figure 10: Longitudinal (a) tensile and (b) compressive strain distributions along CP and PFJ

422 The modification of the pipeline deformed shape due to faulting effected by the
 423 integration of flexible joints (Fig. 7) has also some effect on the soil response due to pipeline
 424 movement in the trench. This is depicted by the frictional soil force distribution along CP and
 425 PFJ (Fig. 11a), showing a minor increase in the soil plastification length around the fault
 426 vicinity, while increase of the soil plastification length regarding the lateral soil response is
 427 observed for PFJ in Fig. 11b.



428

429

(a)

(b)

430 Figure 11: (a) Frictional soil force and (b) lateral soil force distributions along CP and PFJ

431

432 4. PARAMETRIC STUDIES

433 4.1 Pipeline under bending and tension

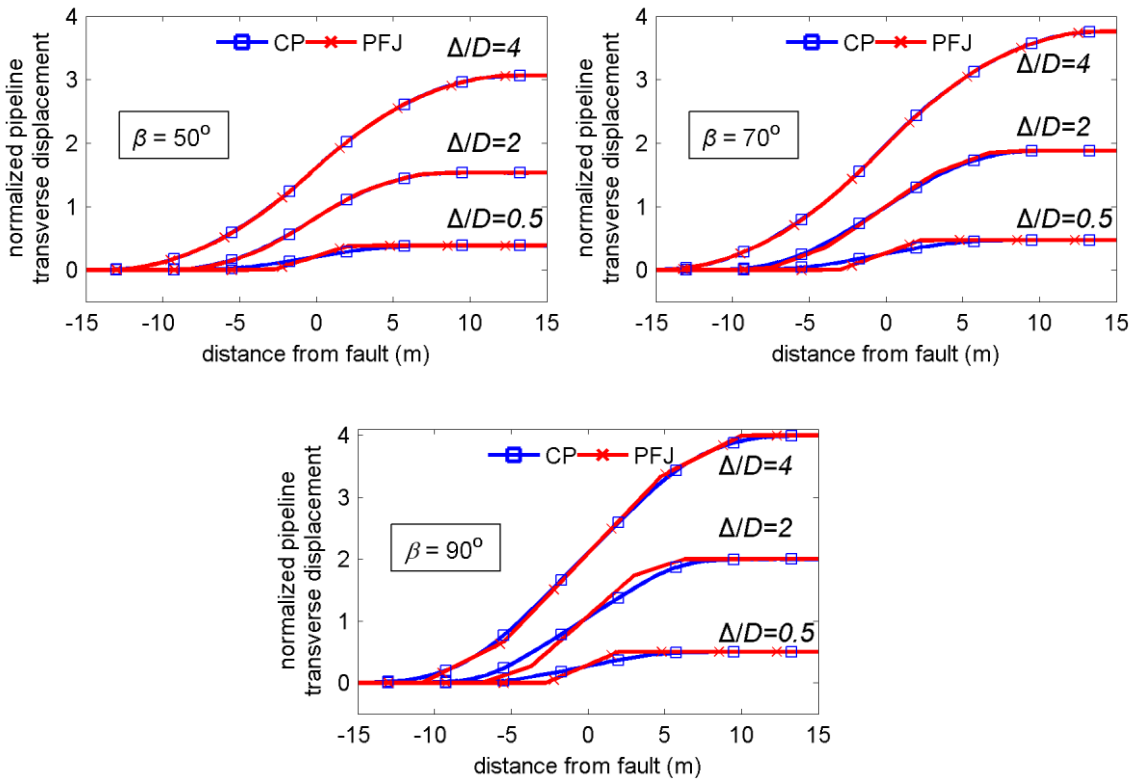
434 The pipeline – fault crossing angle β is a dominant parameter of the pipeline
 435 mechanical behavior due to strike-slip faulting. The major effect of angle β is its influence on

436 the relationship of pipe developing tension and bending moment with respect to the fault
437 movement magnitude. When angle β tends to 90° , the pipeline intercepts the fault plane
438 nearly perpendicularly and bending dominates the response. Tension is the primary stress-
439 state when angle β is lower, as the pipeline tends to become parallel to the fault trace. It is
440 thus essential to investigate the impact of the crossing angle β on the response of pipelines
441 with flexible joints. The integrated joints act as internal hinges in the structural system and
442 consequently their efficiency depends on the degree of flexural versus axial response. Within
443 this framework, a continuous pipeline and the corresponding pipeline with four flexible joints
444 are investigated. The joints are located in each case according to the procedure described in
445 section 3.1. Three characteristic crossing angles are considered, namely $\beta = 50^\circ$, $\beta = 70^\circ$
446 and $\beta = 90^\circ$. The maximum fault movement is assumed equal to $\Delta/D = 4$.

447 The displacements of the continuous pipeline (CP) and the pipeline with four flexible
448 joints (PFJ) are illustrated in Fig. 12, where on the horizontal axis the distance from the fault
449 trace is presented and on the vertical axis the normalized pipeline displacement with respect
450 to pipe diameter is shown. Three indicative cases regarding the fault displacement are
451 illustrated, namely $\Delta/D = 0.5$, $\Delta/D = 2$ and $\Delta/D = 4$, to demonstrate the effect of the fault
452 offset magnitude. In all cases the joint angular demand is well below the 40° capacity, as the
453 highest joint rotation reported equals 8.10° . Increasing fault offset and decreasing angle β
454 lead to more intense pipe tension than bending and consequently the differences between
455 the CP and the PFJ deformations tend to be negligible.

456 The effect of angle β on the pipe response is clearly demonstrated through the
457 comparison of developing axial forces and bending moments on CP and PFJ in Fig. 13 and
458 Fig. 14, respectively. The maximum developing axial force (N_{max}) with respect to the fault
459 offset (Δ/D) is depicted in Fig. 13 for three different crossing angles β . The major outcome is
460 that N_{max} is proportional to fault offset. Additionally, as angle β increases to $\beta = 90^\circ$, more
461 tension is developed in PFJ than in CP. The maximum developing bending moment (M_{max})
462 with respect to the fault offset (Δ/D) is illustrated in Fig. 14 for three different crossing angles
463 β . The efficiency of the integrated hinged joints increases as angle β increases and the

464 pipeline crosses the fault trace close to perpendicularly. Another aspect is that the increasing
465 fault offset leads to the decrease of the difference between the M_{\max} of the CP and the PFJ.
466 At the same time, as angle β decreases, tension dominates the pipe behavior and this
467 difference is almost eliminated.



468

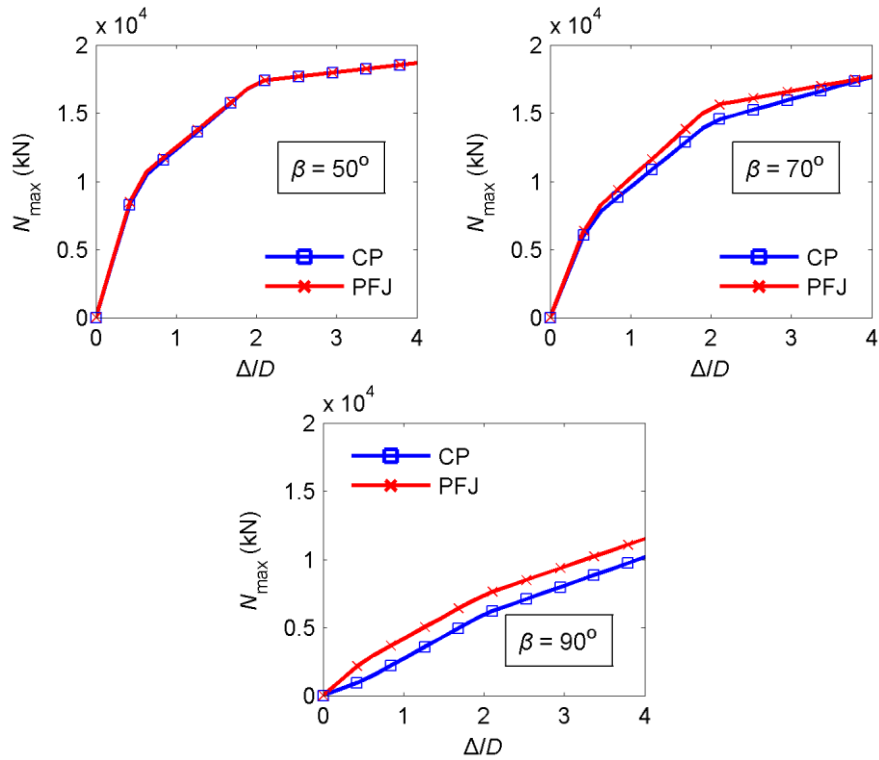
469

470

471

472

Figure 12: CP and PFJ displacements for $\beta = 50^\circ$, $\beta = 70^\circ$ and $\beta = 90^\circ$



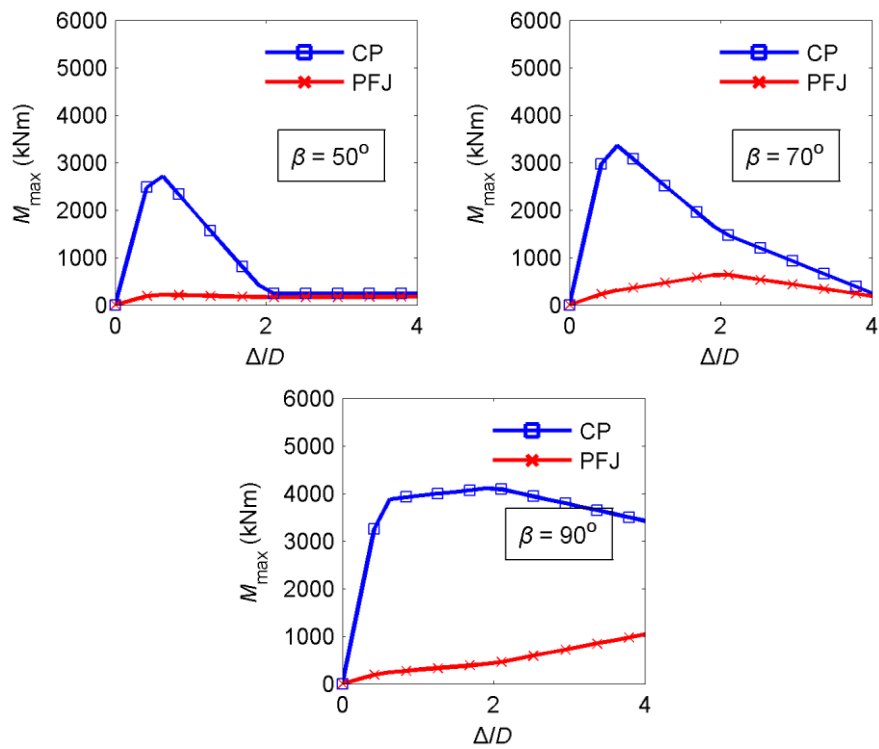
473

474

475

476

Figure 13: Maximum axial force (N_{\max}) of CP and PFJ with respect to fault offset (Δ/D) for $\beta = 50^\circ$, $\beta = 70^\circ$ and $\beta = 90^\circ$



477

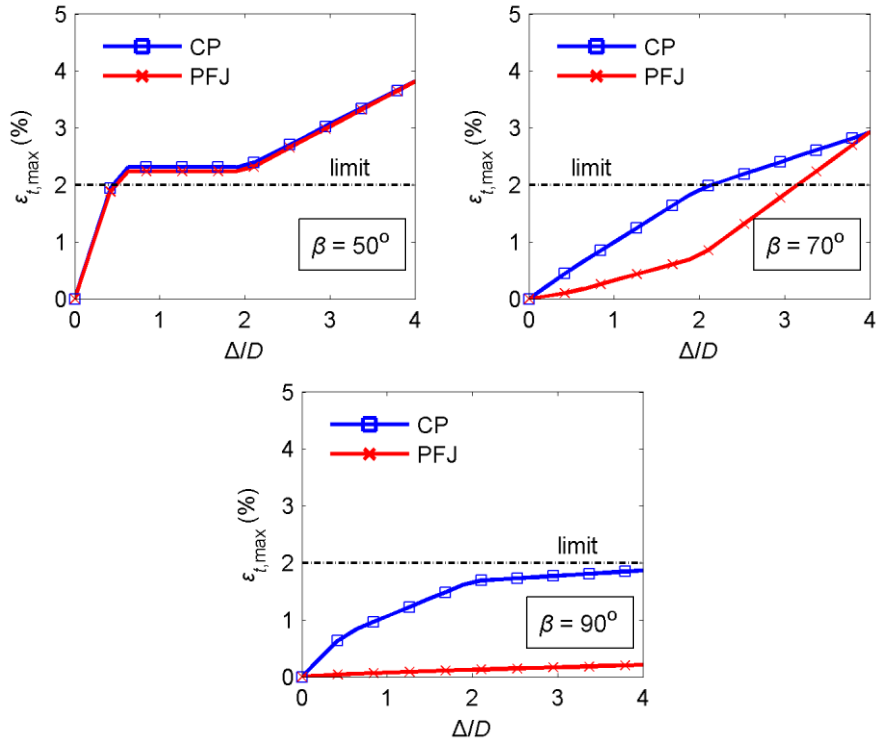
478

479

480

Figure 14: Maximum bending moment (M_{\max}) of CP and PFJ with respect to fault offset (Δ/D) for $\beta = 50^\circ$, $\beta = 70^\circ$ and $\beta = 90^\circ$

481 The maximum developing longitudinal tensile strain ($\epsilon_{t,max}$) of CP and PFJ with respect
482 to the fault offset (Δ/D) is shown in Fig. 15 for the three different crossing angles β . The
483 tensile strain limit of 2% is also presented with a dashed straight line. The development of
484 tensile strains is directly dependent on the crossing angle β . Thus, the decrease of β
485 increases the importance of tension and thereby in case of $\beta = 50^\circ$, joints do not provide
486 strain reduction. It is noted that within a range of fault displacement ($0.5 \leq \Delta/D \leq 2$), the rate
487 of strain increase (for both CP and PFJ) is very low due to the transition from dominant
488 flexural to axial pipe behavior, i.e. the bending strains decrease and the axial strains
489 increase with their summation being more or less constant. In the intermediate case of $\beta =$
490 70° , joints sufficiently prevent tensile fracture by “keeping” strains below the code-based
491 limit, up to $\Delta/D \approx 3$. For larger imposed displacements the pipe stretching dominates and the
492 entailing tension cancels the joint’s efficiency in strain reduction. The maximum tensile strain
493 decrease is achieved for $\beta = 90^\circ$, which is in general the most desirable case for a safe and
494 economically efficient design of a pipeline – fault crossing. The maximum developing
495 compressive strains ($\epsilon_{c,max}$) of CP and PFJ with respect to fault offset are presented in Fig.
496 16 for the same three cases of angle β . Results reveal that pipelines with flexible joints
497 develop very low, almost negligible, compressive strains, hence the potential of local
498 buckling is avoided in all cases.



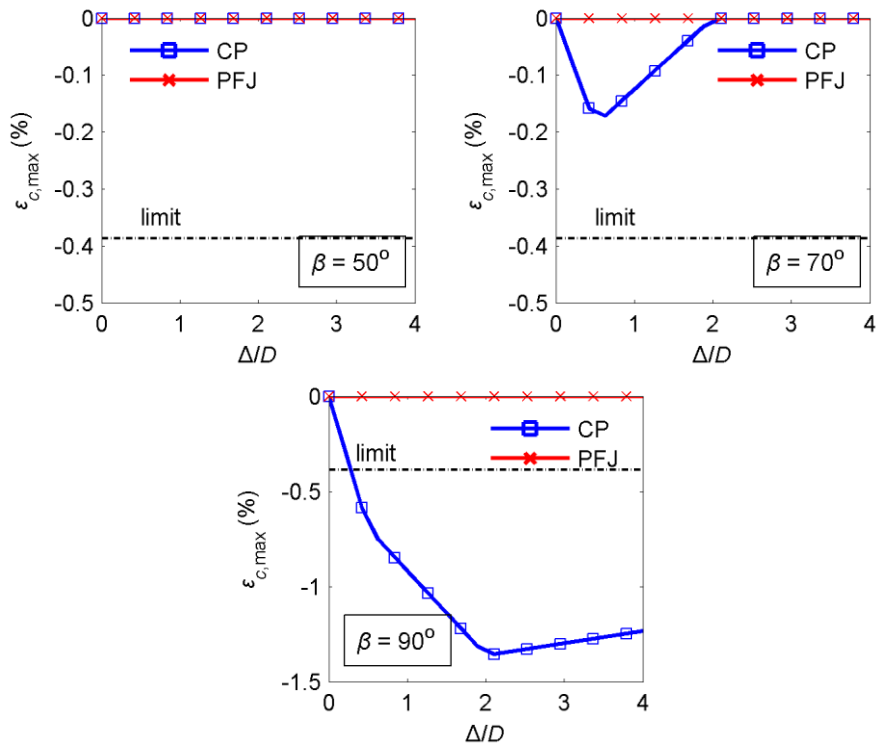
499

500

501

502

Figure 15: Maximum longitudinal tensile strain ($\epsilon_{t,max}$) of CP and PFJ with respect to fault offset (Δ/D) for $\beta = 50^\circ$, $\beta = 70^\circ$ and $\beta = 90^\circ$



503

504

505

506

Figure 16: Maximum longitudinal compressive strain ($\epsilon_{c,max}$) of CP and PFJ with respect to fault offset (Δ/D) for $\beta = 50^\circ$, $\beta = 70^\circ$ and $\beta = 90^\circ$

507 The numerical evaluation of pipelines with flexible joints crossing a strike-slip fault with
508 angle β equal or lower to 90° indicates that the introduction of joints is in most cases a very
509 effective countermeasure that can notably protect a buried steel pipeline against the
510 consequences of faulting. The joints performance is directly related to the pipe – fault
511 crossing angle. The strain reduction is maximized when the pipeline crosses the fault plane
512 close to $\beta = 90^\circ$. For $\beta < 70^\circ$ in combination with higher fault displacements, joints tend not to
513 contribute to the pipe protection in terms of strain reduction. In such cases, the use of joints
514 that are capable of undergoing some axial displacement, in addition to rotation, would be
515 more beneficial.

516

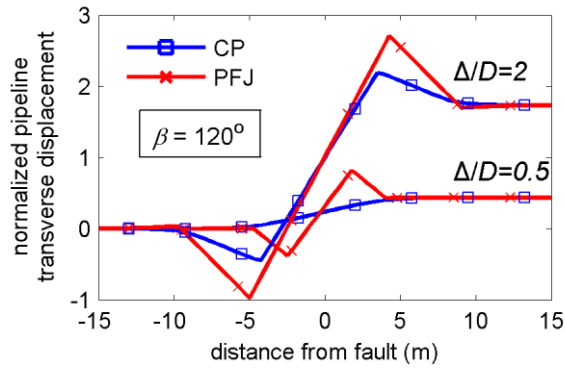
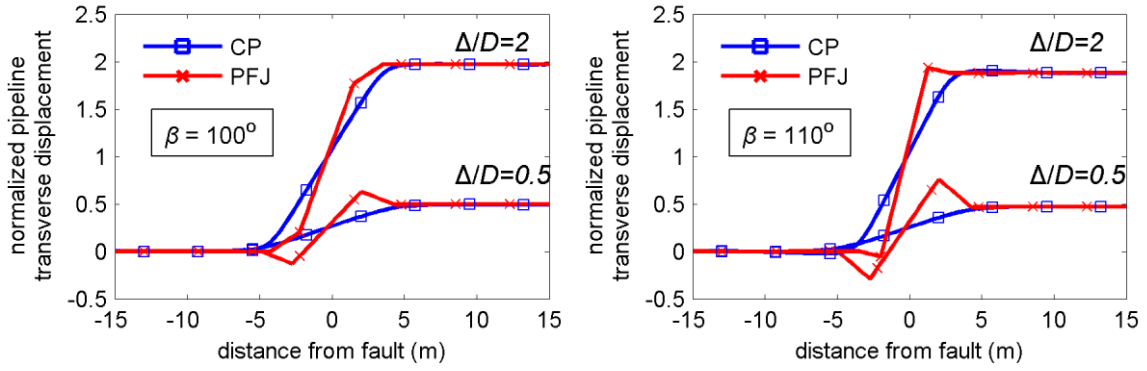
517 **4.2 Pipeline under bending and compression**

518 While in case of tension pipe integrity can rely on the steel post-yielding strength, in
519 case of compression local buckling can lead to pipe failure at much lower absolute strain
520 levels. Pertinent standards and provisions, as well as engineering practice, suggest to avoid
521 crossing angles $\beta > 90^\circ$, which would result in the development of bending and excessive
522 compression along the pipe. Crossing angles $\beta > 90^\circ$ might, however, be unavoidable due to
523 limitations encountered in the route selection procedure, or it might occur unintentionally,
524 due to insufficient data regarding the fault behavior. The repercussions of such values of
525 angle β on the pipeline response are again investigated through the numerical evaluation of
526 a continuous pipeline (CP) and a pipeline with four flexible joints (PFJ). The pipes are
527 assumed to intercept the fault plane with angles $\beta = 100^\circ$, $\beta = 110^\circ$ and $\beta = 120^\circ$, selected in
528 light that $\beta > 90^\circ$ is an undesirable design approach and thus higher values would be
529 unrealistic in common design practice. The maximum fault offset is assumed to be $\Delta/D = 2$.

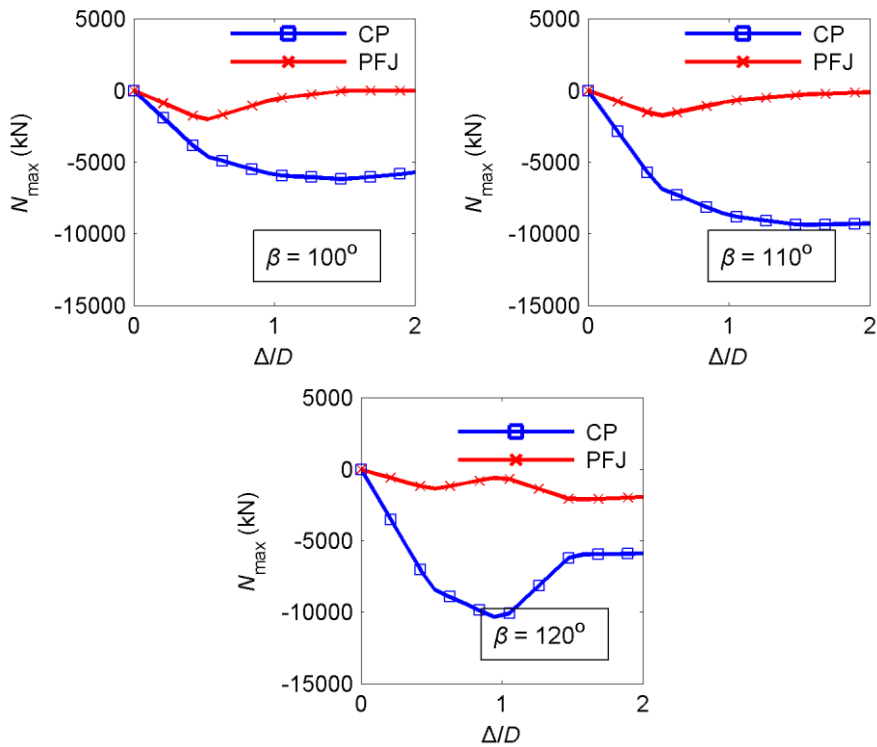
530 Indicative results regarding the CP and PFJ displacements for all crossing angles are
531 illustrated in Fig. 17, where the distance from the fault trace is presented on the horizontal
532 axis and the normalized transverse pipe displacement on the vertical axis. The comparison
533 of pipe displacements between cases of $\beta < 90^\circ$ and $\beta > 90^\circ$ reveals that compression
534 magnifies the difference between CP and PFJ displacements due to pipe shortening and

535 intense joint rotation. The intense PFJ displacement compared to CP is the cause of the
536 effectiveness of joints in all cases of $\beta > 90^\circ$, as will be shown later. The maximum joint
537 rotation reported in the results equals 39.9° and consequently the PFJ is severely deformed,
538 having practically encountered global instability. It is therefore necessary to pay special
539 attention to the angular capacity of the joint in terms of providing rotational capacity
540 “overstrength”.

541 The introduction of flexible joints leads in general to a significant decrease of the pipe
542 stress-state in terms of developing axial forces, bending moments and longitudinal strains for
543 the crossing angles $\beta = 100^\circ$, $\beta = 110^\circ$ and $\beta = 120^\circ$ under consideration. In more details, the
544 maximum developing compressive force (N_{\max}) with respect to the fault offset is depicted in
545 Fig. 18. Axial compressive forces of PFJ are much lower than CP due to the pipe
546 deformation. The maximum developing bending moments (M_{\max}) with respect to the fault
547 offset (Δ/D) are presented in Fig. 19, illustrating that bending moments of PFJ are several
548 times lower than those of CP. Coming to the safety checking, the maximum tensile strains
549 ($\epsilon_{t,\max}$) and compressive strains ($\epsilon_{c,\max}$) of CP and PFJ with respect to fault offset (Δ/D) are
550 shown in Fig. 20 and Fig. 21, respectively, along with code-based strain limits. Tensile
551 strains increase as the fault offset increases, but in general they decrease as the crossing
552 angle increases due to the higher compression. In either case, tensile strains of PFJ are
553 almost negligible, thus ensuring the integrity of girth welds. Regarding, then, the
554 compressive strains, one can notice (Fig. 21) that the CP is going to suffer severe damage,
555 mainly due to local buckling, even for relatively small fault offset ($\Delta/D < 0.5$). Developing
556 compressive strains of CP for $\Delta/D > 0.5$ are too high in practice to be fairly compared with
557 the corresponding ones of PFJ in the same chart for $0 \leq \Delta/D \leq 2$. It then follows that flexible
558 joints in buried pipelines with $\beta > 90^\circ$ can very efficiently protect the pipe against local
559 buckling in all cases under consideration.

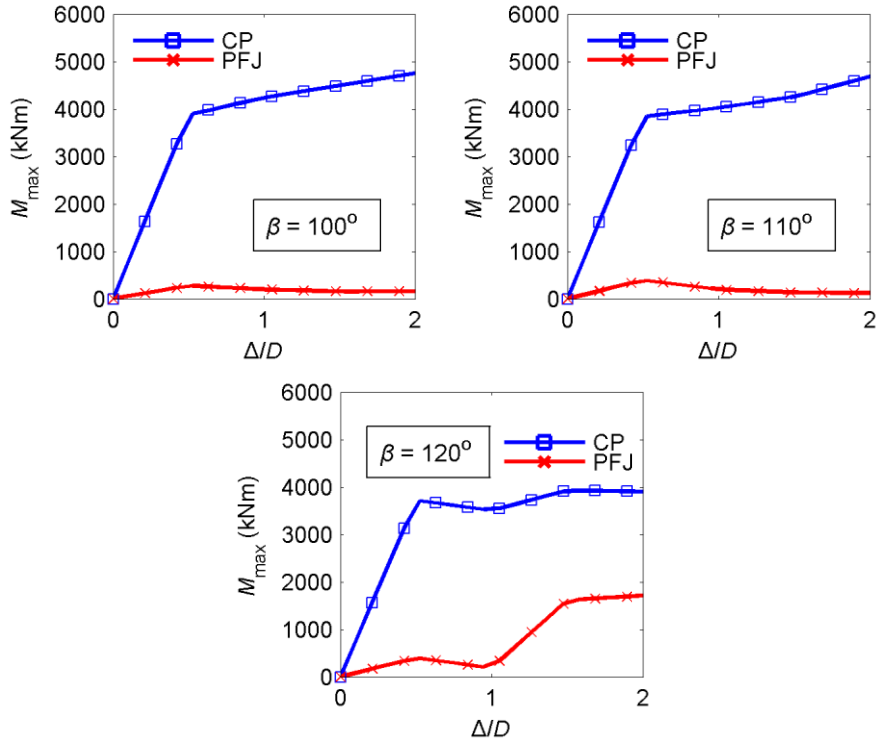


562 Figure 17: CP and PFJ displacements for $\beta = 100^\circ$, $\beta = 110^\circ$ and $\beta = 120^\circ$



565 Figure 18: Maximum axial force (N_{\max}) of CP and PFJ with respect to fault offset (Δ/D) for $\beta =$

566 100° , $\beta = 110^\circ$ and $\beta = 120^\circ$



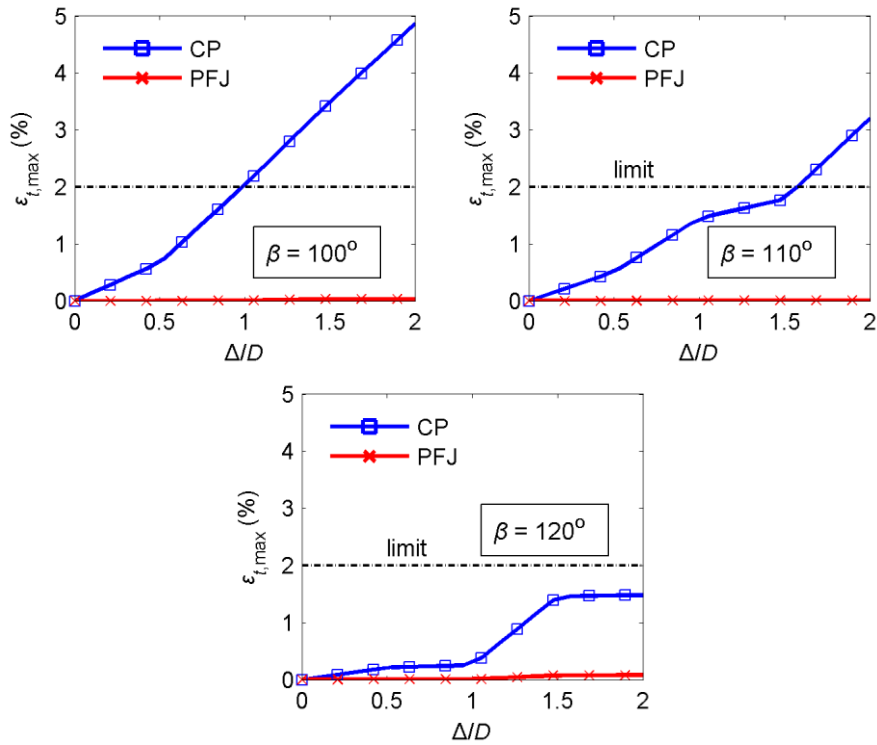
567

568

569 Figure 19: Maximum bending moment (M_{\max}) of CP and PFJ with respect to fault offset (Δ/D)

570

for $\beta = 100^\circ$, $\beta = 110^\circ$ and $\beta = 120^\circ$



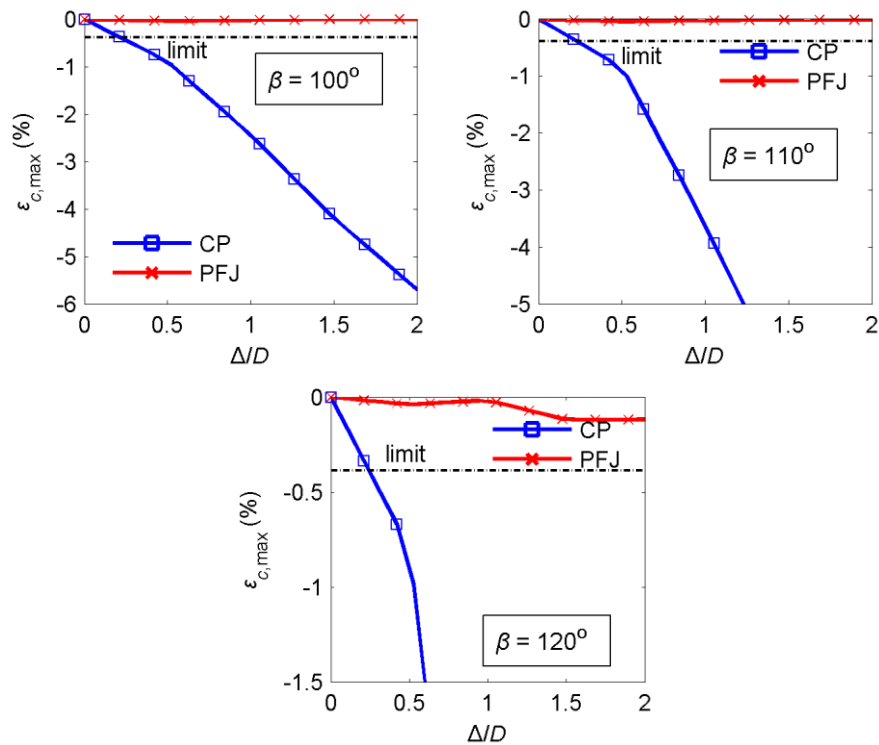
571

572

573 Figure 20: Maximum longitudinal tensile strain ($\epsilon_{t,\max}$) of CP and PFJ with respect to fault

574

offset (Δ/D) for $\beta = 100^\circ$, $\beta = 110^\circ$ and $\beta = 120^\circ$



575

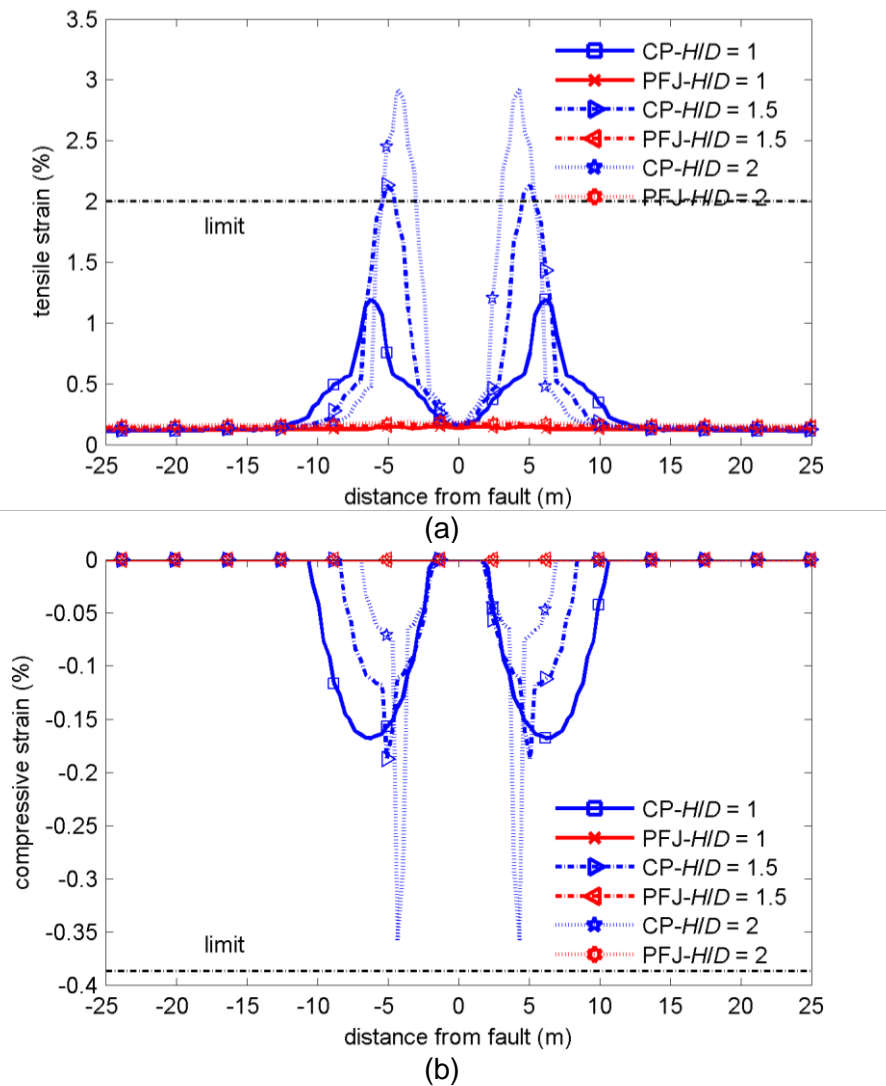
576

577 Figure 21: Maximum longitudinal compressive strain ($\epsilon_{c,max}$) of CP and PFJ with respect to
 578 fault offset (Δ/D) for $\beta = 100^\circ$, $\beta = 110^\circ$ and $\beta = 120^\circ$

579 **4.3 Effect of burial depth**

580 Oil and gas pipelines are usually embedded in a trench to be protected against
 581 corrosion and third party damage. Soil response to any pipe movement in the trench is
 582 related to the pipe burial depth that defines the level of soil pressure acting on the pipe. In
 583 numerical modeling, increase of burial depth leads to stiffer soil springs and consequently
 584 pipeline movement in the trench becomes more difficult, thus the pipe developing stress-
 585 state is higher. It is therefore meaningful to investigate the effect of burial depth on the strain
 586 reduction efficiency of flexible joints. Engineering and constructional practice suggest that
 587 the burial depth equals about one to two times the pipe diameter in fault crossings. The
 588 pipeline under investigation is considered to intercept a strike-slip fault with crossing angle β
 589 $= 70^\circ$ and subjected to $\Delta/D = 1$ of fault offset, representing a typical case. Three cases of
 590 burial depths for the continuous pipeline (CP) and the corresponding pipeline with flexible
 591 joints (PFJ) are considered, namely $H/D = 1$, $H/D = 1.5$ and $H/D = 2$, where H is the soil
 592 height above the top of the pipe.

593 Pipeline response is examined through the longitudinal tensile and compressive strain
 594 distributions (Fig. 22). The increase of burial depth leads to strain increase for the
 595 continuous pipeline, as expected due to stiffer soil springs, and threatens its integrity in
 596 terms of exceeding code-based tensile strain limit. On the contrary, nearly negligible
 597 differences are reported for PFJ cases regarding the strain reduction on the steel pipe parts
 598 due to the integration of flexible joints. The effect of burial depth on joints efficiency can be
 599 thus described as negligible.



600
601

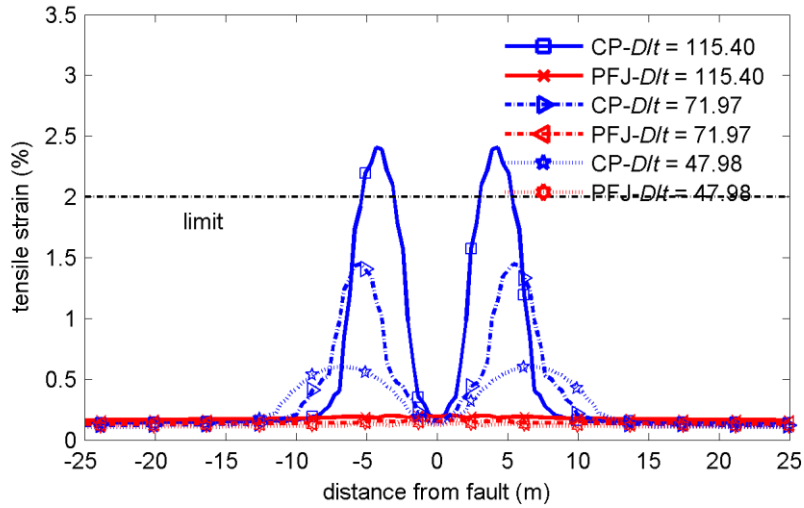
602
603
604
605
606
607
608

Figure 22: (a) Tensile and (b) compressive strain distributions of CP and PFJ for various burial depths (H/D)

609 **4.4 Effect of D/t ratio**

610 The geometry of the pipeline cross-section is defined through the process analysis of
611 the pipeline system and in particular pipe diameter (D) and wall thickness (t) are related to
612 operating flow, temperature, pressure, etc. The diameter over thickness ratio (D/t) plays a
613 dominant role in the pipeline response and especially on buckling behavior, as it defines the
614 pipe slenderness. Shallowly buried pipelines with low D/t under compression may buckle
615 upwards as a beam, while deeper buried pipes with higher D/t tend to buckle locally [55].
616 The D/t ratio is therefore a significant parameter, whose effect on pipelines with flexible joints
617 is hereafter examined by considering CP and PFJ crossing a strike-slip fault with angle $\beta =$
618 70° and subjected to $\Delta/D = 1$ of fault movement. Pipe diameter is considered to be constant
619 $D = 914\text{mm}$, while three cases of commercial thickness values are considered, namely $t =$
620 7.92mm , $t = 12.70\text{mm}$ and $t = 19.05\text{mm}$. The corresponding ratios are then $D/t = 115.40$, D/t
621 $= 71.97$ and $D/t = 47.98$.

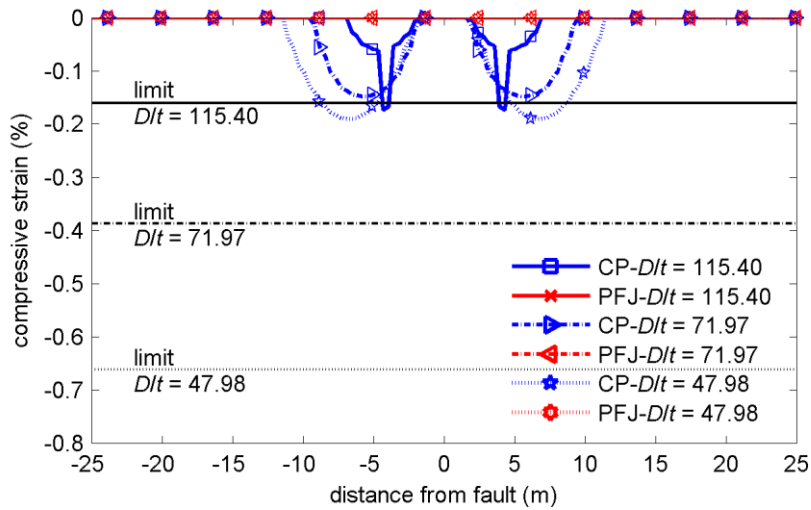
622 The tensile and compressive strain distributions for all cases are illustrated in Fig. 23.
623 The first important observation for CP is that higher D/t ratios increase the structure's
624 slenderness and consequently higher strains are developed due to reduced stiffness. The
625 integration of flexible joints between the pipe adjacent parts transforms the structural system
626 from continuous to segmented and the effect of ratio D/t is almost eliminated. The latter is
627 verified by the strain distributions of PFJs that indicate almost no interaction between the
628 ratio D/t and flexible joints effectiveness in terms of reducing strains.



629

630

(a)



631

632

(b)

633 Figure 23: (a) Tensile and (b) compressive strains distributions of CP and PFJ for various D/t
 634 ratios

635

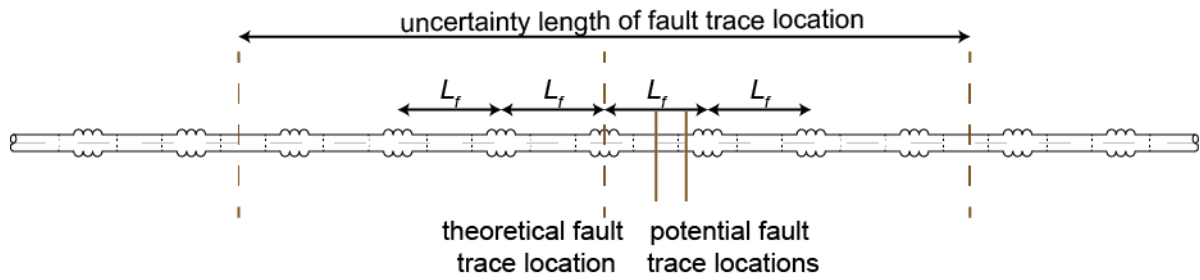
636 **5. UNCERTAINTY REGARDING FAULT TRACE**

637 The analysis of buried pipeline – fault crossing is usually based on the assumption of a
 638 planar fault, intercepting the pipeline at a specific location. Optimum locations of hinged
 639 joints have then been defined in the previous sections with respect to this assumption.
 640 These approaches, however, can be violated in nature by the native soil conditions. Soil
 641 stratigraphy may affect the direction of rupture propagation to the surface. In case the native

642 soil conditions are rocky, the rupture propagation from the underlying bedrock to the ground
643 surface may not be disturbed and thus the planar fault assumption is sufficiently accurate.
644 Nevertheless, the upper soil layers are usually earth fill with inhomogeneous properties (e.g.
645 alluvial deposits) that can alter the rupture propagation to the surface. This can result to a
646 shift of the fault trace from where it is expected to appear on the ground surface. The fault
647 trace uncertainty is not usually considered in the pipe – fault crossing analysis, and in
648 practice design engineers deal with the fault trace uncertainty by applying seismic
649 countermeasures over the entire pipe length, in which the fault trace may be encountered.
650 The latter is estimated by seismological, geological and geotechnical surveys and can range
651 from a few meters to a few hundred meters. Regarding, then, the application of flexible joints
652 as mitigating measures by considering the fault trace uncertainty, this same approach has to
653 be adopted. The important question that arises is regarding the optimum configuration of
654 flexible joints, assuming that joints shall be integrated in the pipeline at equal distances for
655 practical and constructional reasons. In order to address this task, the following procedure is
656 proposed:

- 657 – Estimation of the length over which the fault may “appear” on the ground surface.
- 658 – Analysis of a continuous pipeline subjected to the maximum fault offset, as defined by
659 relevant geological and seismological studies of the area, by assuming the theoretical fault
660 trace being located at the middle of the length of uncertainty.
- 661 – Plot of the bending moment distribution of the continuous pipeline and estimation of
662 distance L_j (Fig. 6), which is the distance between the assumed fault trace location and the
663 maximum bending moment location.
- 664 – Integration of a flexible joint at the theoretical fault trace location and consequently at
665 distances equal to L_f on each side of the fault trace, as schematically illustrated in Fig. 24.
666 Additionally, two joints are introduced outside the “borders” of uncertainty area, in order to
667 address the worst case scenario of the fault being activated at the margins of the
668 uncertainty area.

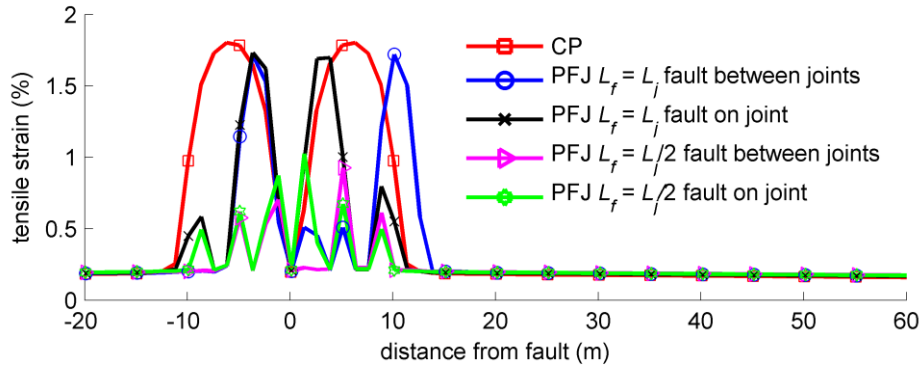
669 – Estimation of the optimum distance L_f , by considering the fault trace being located either
670 between two flexible joints or closer to a joint.



671

672 Figure 24: Configuration of flexible joints over the length of fault trace uncertainty and
673 potential fault trace locations

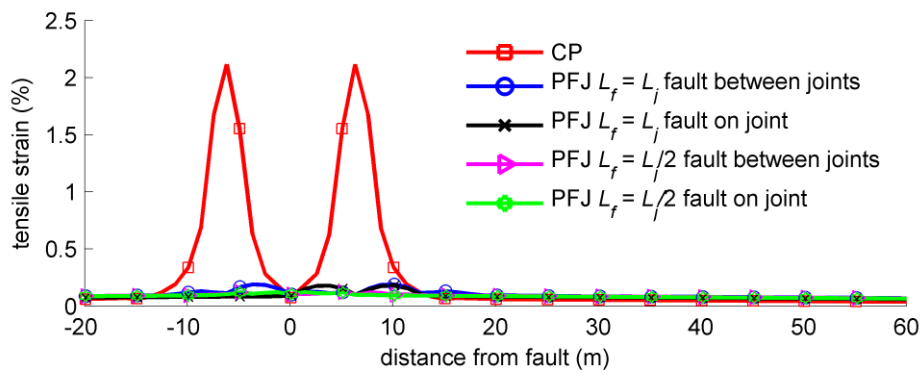
674 An essential part of the procedure regarding the integration of flexible joints over the length
675 of fault trace uncertainty is the estimation of distance L_f . Taking into account that the
676 optimum configuration of joints for a given fault trace location is at distance $L_f/2$ between two
677 joints and the fault trace, analyses are carried out consequently, assuming that $L_f = L_j/2$ or L_f
678 $= L_j$. The potential fault trace locations for each case are depicted in Fig. 24. The pipeline
679 with flexible joints (PFJ) is subjected to strike-slip fault offset of magnitude $\Delta/D = 2$ and the
680 pipeline – fault crossing angle is assumed to be equal to $\beta = 70^\circ$ and $\beta = 90^\circ$. The
681 continuous pipeline (CP) is also considered for reference. The distributions of tensile strains
682 along the pipeline are depicted in Fig. 25. It is observed that regardless of the fault trace
683 location, the optimum configuration of flexible joints in terms of reducing the developing
684 tensile strains is at distance $L_f = L_j/2$ for crossing angle $\beta = 70^\circ$. On the contrary, for $\beta = 90^\circ$ it
685 is observed that both configurations, namely $L_f = L_j$ and $L_f = L_j/2$, are roughly equally efficient
686 and thus for pipeline – fault crossing close or equal to perpendicularity it is suggested that
687 joints are integrated at distance $L_f = L_j$ in order to minimize the cost. It is noted that if there is
688 uncertainty regarding the pipe – fault crossing angle β , then joints should be integrated at
689 distance $L_f = L_j/2$ in order to address the worst case scenario.



690

691

(a)



692

693

(b)

694

Figure 25: Tensile strain distributions for crossing angle (a) $\beta = 70^\circ$ and (b) $\beta = 90^\circ$ considering different configuration of flexible joints and fault trace being located either between two adjacent joints or at a joint

696

697

698 6. SUMMARY AND CONCLUSIONS

699

700

701

702

703

704

705

706

Buried steel pipelines with flexible joints subjected to strike-slip fault offset have been investigated using advanced numerical modeling and nonlinear analysis, employing the beam-type model. The flexible joints of hinged bellow-type are proposed as innovative mitigating measures against the consequences of faulting on the pipeline. They are introduced in continuous pipes to concentrate strains at the joints and retain the steel pipe parts virtually unstressed. The presented numerical study stands as a preliminary feasibility study of the effectiveness of joints in terms of reducing the developing longitudinal tensile and compressive strains and consequently reducing the risk of pipe failure. Taking also into

707 account that hinged bellow-type flexible joints have not been used before as seismic
708 countermeasures in buried pipes subjected to fault rupture, it is emphasized that
709 technological and practical aspects of such joints must be solved before actual application.
710 Thus, by demonstrating and quantifying the structural advantages of the proposed approach,
711 the present study aims at motivating further industrial research towards addressing these
712 practical aspects.

713 The optimum number and location of flexible joints on the pipeline were examined in
714 case of strike-slip faulting, while the main parameters affecting their efficiency were
715 investigated, namely pipeline – fault crossing angle, fault offset magnitude, burial depth and
716 ratio D/t . Additionally, the uncertainty on fault trace was addressed and suggestions were
717 formulated for practical applications. The main conclusions of the present study can be
718 summarized as follows:

- 719 1. Metallic hinged bellow-type flexible joints are the appropriate type of commercial flexible
720 joints for buried pipeline – fault crossing applications. Such joints exhibit low rotational
721 stiffness, while the axial and lateral relative movements are constrained, to withstand
722 large internal pressure and pipe movements due to faulting.
- 723 2. The introduction of flexible joints transforms the pipeline structural system from
724 continuous to segmented. Numerical results indicated significant strain reduction due to
725 the integration of joints, as imposed deformation is now absorbed by rotation at the joints.
- 726 3. Parametric studies carried out showed that the joints' efficiency is maximized for crossing
727 angles β closer to 90° , where bending moment dominates the pipeline behavior. As angle
728 β decreases and fault offset increases, tension dominates the pipe behavior and joints'
729 contribution to strain reduction deteriorates. Thus, use of commercial hinged flexible joints
730 is recommended for crossing angles β larger than 70° .
- 731 4. For crossing angle $\beta > 90^\circ$ joints can ensure the pipe integrity. The extensive deformation
732 relieves the pipe from the compressive axial force. However, special attention has to be
733 paid on the joint's angular capacity, as very high rotation is expected.

734 5. The performance of flexible joints in reducing longitudinal tensile and compressive strains
735 has been shown to be independent of D/t ratio and burial depth H , as joints' efficiency is
736 independent of pipe cross-section geometry and soil properties.

737 6. Geological conditions and soil properties at the fault crossing site may introduce an
738 uncertainty regarding the fault trace location on the ground surface. To account for this
739 uncertainty, joints should be integrated along the entire pipeline length, where fault trace
740 might appear on the ground surface, which is also the case when other mitigating
741 measures are used. For angle β near 90° the optimum distance between joints is equal to
742 distance L_j between the assumed fault trace and the location of maximum bending
743 moment in a continuous pipeline. For smaller angles β approaching 70° , smaller distance
744 between joints is recommended, in the order of $L_j/2$.

745 In conclusion, the introduction of commercial hinged bellow-type flexible joints in
746 continuous buried steel pipes has been shown leading to significant strain reduction and
747 consequently protection of the pipeline from fault offset. Hinged joints were examined in
748 case of strike-slip faulting, but the encouraging results indicate their potential applicability in
749 cases of normal or reverse faulting as well. As a final comment, fault offset is in nature three-
750 dimensional and in such case hinged joints with biaxial angular capability (Gimbal type joint)
751 should be implemented.

752

753 **ACKNOWLEDGMENTS**

754 This research has been co-financed by the European Union (European Social Fund – ESF)
755 and Hellenic National Funds through the Operational Program “Education and Lifelong
756 Learning” (NSRF 2007-2013) – Research Funding Program “Aristeia II”, project
757 “ENSSTRAM - Novel Design Concepts for Energy Related Steel Structures using Advanced
758 Materials”, grant number 4916.

759

760 **REFERENCES**

- 761 [1] O'Rourke MJ, Liu X. Seismic design of buried and offshore pipelines. Monograph No. 4".
762 Buffalo: Multidisciplinary Center for Earthquake Engineering Research; 2012.
- 763 [2] Nakata T, Hasuda K. Active fault I 1995 Hyogoken Nanbu earthquake. Kagaku 1995;
764 65:127-142.
- 765 [3] Earthquake Engineering Research Institute. Kocaeli, Turkey Earthquake of August 17.
766 Pasadena: EERI Special Earthquake Report; 1999.
- 767 [4] Takada S, Nakayama M, Ueno J, Tajima C. Report on Taiwan Earthquake. Kobe:
768 RCUSS, Earthquake Laboratory of Kobe University; 1999.
- 769 [5] Newmark NM, Hall WJ. Pipeline design to resist large fault displacement. Proceedings of
770 U.S. National Conference on Earthquake Engineering, Michigan, 18-20 June 1975.
- 771 [6] Kennedy RP, Chow AW, Williamson RA. Fault movement effects of buried oil pipeline.
772 ASCE J Transp Eng 1977;103:617-33.
- 773 [7] Kennedy RP, Kincaid RH. Fault crossing design for buried gas oil pipeline. In: Proceeding
774 of ASME, PVP Conference, vol. 77; 1983. p. 1-9.
- 775 [8] Wang LRL, Yeh YA. A refined seismic analysis and design of buried pipelines subjected
776 to vertical fault movement. Earthq Eng Struct Dyn 1985;13:75-96.
- 777 [9] Vougioukas EA, Theodossis C, Carydis PG. Seismic analysis of buried pipelines
778 subjected to vertical fault movement. ASCE J Tech Counc 1979;105(TCI):432-41.
- 779 [10] Wang LRL, Wang LJ. Parametric study of buried pipelines due to large fault movement.
780 In: Proceedings of ASCE, TCLEE, vol. 6; 1995. P. 152-9.
- 781 [11] Takada S, Hassani N, Fukuda K. A new proposal for simplified design of buried steel
782 pipes crossing active faults. Earthq Eng Struct Dyn 2001;30(2001):1243-57.
783 DOI: 10.1002/eqe.62
- 784 [12] Karamitros DK, Bouckovalas GD, Kouretzis GD. Stress analysis of buried steel pipelines
785 at strike-slip fault crossings. Soil Dyn Earthq Eng 2007;27:200-11. DOI:
786 10.1016/j.soildyn.2006.08.001

787 [13] Karamitros DK, Bouckovalas GD, Kouretzis GD, Gkesouli V. An analytical method for
788 strength verification of buried steel pipelines at normal fault crossings. *Soil Dyn Earthq Eng*
789 2011;31:1452-64. DOI: 10.1016/j.soildyn.2011.05.012

790 [14] Trifonov OV, Cherniy VP. A semi-analytical approach to a nonlinear stress-strain
791 analysis of buried steel pipelines crossing active faults. *Soil Dyn Earthq Eng* 2010;30:1298-
792 308. DOI: 10.1016/j.soildyn.2010.06.002

793 [15] Trifonov OV, Cherniy VP. Elastoplastic stress-strain analysis of buried steel pipelines
794 subjected to fault displacement with account for service loads. *Soil Dyn Earthq Eng*
795 2012;33(1):54-62. DOI: 10.1016/j.soildyn.2011.10.001

796 [16] Ariman T, Lee BJ. Tension/Bending behavior of buried pipelines under large ground
797 deformation in active faults. In: U.S. Conference on Lifeline Earthquake Engineering, ASCE
798 Technical Council on Lifeline Earthquake Engineering, vol. 4; 2001; p. 226-33.

799 [17] Joshi S, Prashant A, Deb A, Jain SK. Analysis of buried pipelines subjected to reverse
800 fault motion. *Soil Dyn Earthq Eng* 2011;31:930-40. DOI: 10.1016/j.soildyn.2011.02.003

801 [18] Uckan E, Akbas B, Shen J, Rou W, Paolacci F, O'Rourke M. A simplified analysis model
802 for determining the seismic response of buried steel pipes at strike-slip fault crossings. *Soil*
803 *Dyn Earthq Eng* 2015;75:55-65. DOI: 10.1016/j.soildyn.2015.03.001

804 [19] Comité Européen de Normalisation. Eurocode 8, Part 4: Silos, tanks and pipelines. CEN
805 EN 1998-4, Brussels, Belgium; 2006.

806 [20] ALA American Lifelines Alliance. Guideline for the design of buried steel pipe – July
807 2001 (with addenda through February 2005). American Society of Civil Engineers, New
808 York, USA; 2005.

809 [21] American Society of Civil Engineers. Guidelines for the seismic design of oil and gas
810 pipeline systems. Committee on gas and liquid fuel life-lines, technical council on lifeline
811 earthquake engineering, ASCE, New York, USA; 1984.

812 [22] Kokavessis NK, Anagnostidis GS. Finite element modeling of buried pipelines subjected
813 to seismic loads: soil structure interaction using contact elements. In: Proceedings of ASME,
814 PVP Conference, Vancouver; 2006.

815 [23] Odina L, Tan R. Seismic fault displacement of buried pipelines using continuum finite
816 element methods. In: Proceedings of the ASME 2009 28th International Conference on
817 Ocean, Offshore and Arctic Engineering, Honolulu; 2009.

818 [24] Vazouras P, Karamanos SA, Dakoulas P. Finite element analysis of buried steel
819 pipelines under strike-slip fault displacements. *Soil Dyn Earthq Eng* 2010;30(11):1361-76.
820 DOI: 10.1016/j.soildyn.2010.06.011

821 [25] Vazouras P, Karamanos SA, Dakoulas P. Mechanical behavior of buried steel pipes
822 crossing active strike-slip faults. *Soil Dyn Earthq Eng* 2012;41:164-80. DOI:
823 10.1016/j.soildyn.2012.05.012

824 [26] Vazouras P, Dakoulas P, Karamanos SA. Pipe-soil interaction and pipeline performance
825 under strike-slip fault movements. *Soil Dyn Earthq Eng* 2015;72:48-65. DOI:
826 10.1016/j.soildyn.2015.01.014

827 [27] Zhang J, Liang Z, Han CJ. Buckling behavior analysis of buried gas pipeline under
828 strike-slip fault displacement. *J Nat Gas Sc Eng* 2014;21:901-28. DOI:
829 10.1016/j.jngse.2014.10.028

830 [28] Trifonov OV. Numerical stress-strain analysis of buried steel pipelines crossing active
831 strike-slip faults with an emphasis on fault modeling aspects. *ASCE J Pipeline Syst Eng*
832 *Pract* 2015;6(1):04014008. DOI: 10.1061/(ASCE)PS.1949-1204.0000177

833 [29] Takada S, Liang JW, Tengyan L. Shell-mode response of buried pipelines to large fault
834 movements. *J Struct Eng* 1998;44A:1637-46.

835 [30] Gantes CJ, Bouckovalas GD. Seismic verification of high pressure natural gas pipeline
836 Komotini – Alexandropoulis – Kipi in areas of active fault crossings. *Struct Eng Int*
837 2013;2:204-8. DOI: 10.2749/101686613X13439149157164

838 [31] Karamanos SA, Keil B, Card RJ. Seismic design of buried steel water pipelines, In:
839 Proceedings of the Pipelines 2014: From Underground to the Forefront of Innovation and
840 Sustainability; 2015 Aug 3-6; Portland, Oregon, USA, p. 1005-19.

841 [32] Mokhtari M, Alavi Nia M. The influence of using CFRP wraps on performance of buried
842 steel pipelines under permanent ground deformations. *Soil Dyn Earthq Eng* 2015;73:29-41.
843 DOI: 10.1016/j.soildyn.2015.02.014

844 [33] Hedge AM, Sitharam TG. Experimental and numerical studies on protection of buried
845 pipelines and underground utilities using geocells. *Geotextiles and Geomembranes*
846 2015;43:372-81. DOI: 10.1016/j.geotexmem.2015.04.010

847 [34] Sim WW, Towhata I, Yamada S, Moinet GJ-M. Shaking table tests modelling small
848 diameter pipes crossing a vertical fault. *Soil Dyn Earthq Eng* 2012;35:59-71. DOI:
849 10.1016/j.soildyn.2011.11.005

850 [35] Monroy-Concha M. Soil restraints on steel buried pipelines crossing active seismic faults
851 [dissertation]. Canada: The University of British Columbia; 2013.

852 [36] Ford DB. Joint design for pipelines subjected to large ground deformations. In:
853 *Proceedings of the ASME 1983 Pressure Vessels and Piping Division Conference*, ASME,
854 New York; 1983: 160–165.

855 [37] Elhmadi K, O'Rourke MJ. Seismic damage to segmented buried pipelines. *Earthq Eng*
856 *Str Dyn* 1990;19:529–539. DOI: 10.1002/eqe.4290190405

857 [38] O'Rourke MJ. Analytical fragility relation for buried segmented pipe. In: *Proceedings of*
858 *the 2009 TCLEE Conference: Lifeline Earthquake Engineering in a Multihazard Enviroment*,
859 ASCE, Oakland, 2009: 771–780.

860 [39] O'Rourke MJ, Ballantyne D. Observations on water system and pipeline performance in
861 the Limon area of Costa Rica due to the April 22, 1991 earthquake. Buffalo: Multidisciplinary
862 Center for Earthquake Engineering Research; 1992.

863 [40] O'Rourke MJ, Liu X. Seismic design of buried and offshore pipelines. Buffalo:
864 Multidisciplinary Center for Earthquake Engineering Research; 2012.

865 [41] O'Rourke MJ, Norberg C. Analysis procedures for buried pipelines subject to
866 longitudinal and transverse permanent ground deformation. In: *Proceedings of the Third*
867 *Japan-U.S. Workshop on Earthquake Resistant Design of Lifelines and Countermeasures*
868 *for Soil Liquefaction*, San Francisco; 1991: 439–453.

869 [42] O'Rourke TD, Trautmann CH. Earthquake ground rupture effects on jointed pipe. In:
870 Proceedings of the Lifeline Earthquake Engineering: The Current State of Knowledge,
871 ASCE, Oakland; 1981: 65–80.

872 [43] Isenberg J, Richardson E. Countermeasures to mitigate damage to pipelines. In:
873 Proceedings of the Second U.S.-Japan Workshop on Liquefaction, Large Ground
874 Deformation and Their Effects on Lifelines, New York; 1989: 468–482.

875 [44] Takada S. Model analysis and experimental study on mechanical behavior of buried
876 ductile iron pipelines subjected to large ground deformations. In: Proceedings of the Eighth
877 World Conference on Earthquake Engineering, San Francisco; 1984: 255–262.

878 [45] Bekki H, Kobayashi K, Tanaka Y, Asada T. Dynamic behavior of buried pipe with flexible
879 joints in liquefied ground. J Japan Sewage Assoc 2002;39:201-8.

880 [46] Melissianos VE, Vamvatsikos D, Gantes CJ. Probabilistic assessment of innovative
881 mitigating measures for buried steel pipeline – fault crossing. In: Proceeding of the ASME,
882 PVP Conference; 2015 Jul 19-23; Boston, Massachusetts, USA.

883 [47] Melissianos VE, Gantes CJ. Failure mitigation of buried steel pipeline under strike-slip
884 fault offset using flexible joints. In: Proceeding of the SECED 2015 Conference: Earthquake
885 Risk and Engineering towards a Resilient World; 2015 Jul 9-10; Cambridge, UK.

886 [48] Abdoun TH, Ha D, O'Rourke MJ, Symans MD, O'Rourke TD, Palmer MC, Stewart HE.
887 Factors influencing the behavior of buried pipelines subjected to earthquake faulting. Soil
888 Dyn Earthq Eng 2009;29:415-27. DOI: 10.1016/j.soildyn.2008.04.006

889 [49] ADINA R & D Inc. Theory and Modeling guide Volume I: ADINA, Report AED 06-7,
890 Watertown, USA; 2006.

891 [50] Peng LC, Peng A. Pipe stress engineering, New York: ASME Press; 2009.

892 [51] EJMA. Standards of the Expansion Joint Manufacturers Association, Inc., 9th Edition.
893 Expansion Joints Manufacturers Association, Inc., Tarrytown, New York, USA; 2008.

894 [52] Bathe KJ, Dvorkin EN. On the automatic solution of nonlinear finite element methods.
895 Computers & Structures 1983;17(5-6):871-79.

896 [53] <http://www.witzenmann.de>

897 [54] <http://www.boagroup.com>

898 [55] Yun HD, Kyriakides S. On the beam and shell modes of buckling of buried pipelines.

899 Soil Dyn Earthq Eng 1990;9(4):179-93. DOI: 10.1016/S0267-7261(05)80009-0